



# Nano-chemo-mechanical signature of conventional oil-well cement systems: Effects of elevated temperature and curing time



Konrad J. Krakowiak<sup>a</sup>, Jeffrey J. Thomas<sup>b</sup>, Simone Musso<sup>b</sup>, Simon James<sup>c</sup>, Ange-Therese Akono<sup>a,1</sup>, Franz-Josef Ulm<sup>a,\*</sup>

<sup>a</sup> Civil and Environmental Engineering Department, Massachusetts Institute of Technology, 77 Massachusetts Avenue, Cambridge, MA 02139-4307, USA

<sup>b</sup> Schlumberger-Doll Research Center, 1 Hampshire St., Cambridge, MA 02139-1578, USA

<sup>c</sup> Schlumberger Riboud Product Center, 1 rue Henri Becquerel, Clamart 92140, France

## ARTICLE INFO

### Article history:

Received 13 March 2014

Accepted 27 August 2014

Available online 29 September 2014

### Keywords:

Thermal treatment (A)

Oil well cement (E)

Microstructure (B)

Mechanical properties (C)

## ABSTRACT

With ever more challenging (T,p) environments for cementing applications in oil and gas wells, there is a need to identify the fundamental mechanisms of fracture resistant oil well cements. We report results from a multi-technique investigation of behavior and properties of API class G cement and silica-enriched cement systems subjected to hydrothermal curing from 30 °C to 200 °C; including electron probe microanalysis, X-ray diffraction, thermogravimetry analysis, electron microscopy, neutron scattering (SANS), and fracture scratch testing. The results provide a new insight into the link between system chemistry, micro-texture and micro-fracture toughness. We suggest that the strong correlation found between chemically modulated specific surface and fracture resistance can explain the drop in fracture properties of neat oil-well cements at elevated temperatures; the fracture property enhancement in silica-rich cement systems, between 110° and 175 °C; and the drop in fracture properties of such systems through prolonged curing over 1 year at 200 °C.

© 2014 Elsevier Ltd. All rights reserved.

## 1. Introduction

Portland cement-based slurries are widely used in oil and gas wells to fill the annular space e.g. between the steel casing and surrounding rock formation [1]. Such cement liners provide structural integrity to the wellbore and also provide zonal isolation to prevent unwanted movement of hydrocarbons, which is critical for environmental safety. The risk of failure can be minimized by a cement sheath performance design that ensures the structural integrity of the well, prevents the formation of fissures at the inner or outer interface of the cement sheath, prevents cracking of the cement, and minimizes the risk of accumulated material damage caused by physicochemical processes, for example undesired phase precipitation or excessive crystal growth, whose effects do not show up until damage has accumulated to a critical extent.

A critical aspect of such a performance design is an adequate fracture resistance of the cement sheath with respect to crack initialization and propagation. This can be achieved through adequate materials design of the slurry chemistry and its components, grounded on an understanding of the physicochemical processes taking place during

hydrothermal curing of the cement system. Such a design should ensure adequate performance over the operational lifespan of the well and beyond.

This paper presents results of experimental work focused on understanding the links between the hydrothermal curing conditions of silica-enriched cement systems, evolution of nano- and micro-texture, and fracture resistance of the cement sheath. Evolution of system mineralogy and phase composition is carried out with standard powder X-ray diffraction, thermal gravimetric analysis, and a new statistical approach for grid electron probe microanalysis (EPMA) on heterogeneous materials. The effect of the pozzolanic reaction between  $\alpha$ -quartz and calcium-rich system components on the phase redistribution and chemistry is traced across a range of curing temperatures from 30 °C to 200 °C via compositional scatter diagrams obtained with grid EPMA. Additionally, the elemental composition of the main calcium silicate hydrate reaction products is determined at each curing temperature, together with a semi-quantitative assessment of their abundance.

The nano-texture of these silica-enriched systems, particularly the degree of coarsening of the fundamental particles or crystals in samples exposed to hydrothermal curing at 175 °C and 200 °C for different durations, is qualitatively assessed using electron microscopy (both scanning and transmission) and small-angle neutron scattering (SANS). The specific surface area is also quantitatively determined with SANS.

The phase chemistry and composition together with the nano-texture information are linked to the fracture toughness of the silica enriched cement systems, using a recently developed micro-scratch

\* Corresponding author. Tel.: +1 617 253 3544.

E-mail addresses: [kjkrak@mit.edu](mailto:kjkrak@mit.edu) (K.J. Krakowiak), [JThomas39@slb.com](mailto:JThomas39@slb.com) (J.J. Thomas), [SMusso@slb.com](mailto:SMusso@slb.com) (S. Musso), [james6@slb.com](mailto:james6@slb.com) (S. James), [aakono@illinois.edu](mailto:aakono@illinois.edu) (A.-T. Akono), [ulm@mit.edu](mailto:ulm@mit.edu) (F.-J. Ulm).

<sup>1</sup> Present Address: University of Illinois at Urbana-Champaign, Civil and Environmental Engineering, 3108 Newmark Civil Engineering Laboratory, 205 N. Mathews Ave. Urbana, IL 61801, USA.

technique, and unconfined compressive strength (UCS) estimated from the Ultrasonic Cement Analyzer (UCA). Both properties are measured with respect to the temperature and duration of hydrothermal curing. Additionally, the microstructure coarsening is also addressed from the point of view of mechanical performance.

A parallel series of tests was performed on control oilwell cement systems without silica, in order to accurately understand the effect of silica incorporation on the micro-texture and microstructure of hydrated cement and its implications on the fracture resistance of cement sheath.

## 2. Materials and methods

### 2.1. Materials and sample synthesis

In this study two oilwell cement systems were investigated: a control system of API class G cement (Dyckerhoff, Wiesbaden, Germany), referred to as the J-series (Table 1), and a silica enriched system referred to as A-series (Table 1). The water-to-cement mass ratio for both systems is  $w/c = 0.45$ . Because of the silica flour incorporated in the A-series samples, in the amount of 35% by weight of cement (bwoc), it has a higher slurry density  $\rho_A = 2030.0 \text{ kg/m}^3$  compared to the control system  $\rho_J = 1890.0 \text{ kg/m}^3$ . The silica flour used in this study is fine ground quartz ( $\alpha$ -quartz), with a particle diameter  $d$  ranging from 10 to  $100 \mu\text{m}$  and a median grain diameter  $d_{50} \approx 20 \mu\text{m}$  (Fig. 1). Other components of the mix include a silicone antifoam agent, a polynaphthalene sulphonate dispersant, and a polymer-based anti-settling agent. The total mass of these additives is less than 1.5% bwoc.

The cement slurries were prepared in accordance with standard procedures recommended in API RP 10B-2 [1,2]. Cement paste samples were cured using a commercial device designed to test oilwell cement slurries under controlled hydrothermal conditions (Ultrasonic Cement Analyzer, Chandler, USA) or in a pressurized curing chamber (A-200). The temperature, pressure, and curing time conditions are given in Table 1. All samples were kept saturated with lime water at all times.

### 2.2. Phase assessment with X-ray powder diffraction

Representative samples for X-ray powder diffraction were prepared for the two investigated oil-well cement systems. Small chunks of approximate weight of 10 g were separated from the mother sample, ground by hand in acetone. The final step included gentle re-grinding and sample homogenization just before the powder was loaded onto the sample holder of the diffractometer. All powder diffraction patterns were collected on a Bruker D8 Advance multipurpose diffractometer with open Eulerian cradle and the Bragg-Brentano geometry, with the Cu-anode (Cu K-alpha  $\lambda = 1.541 \text{ \AA}$ ). Scans were carried out from  $5$  to  $90^\circ/2\theta$ , with a step size of  $0.009^\circ$  and a speed of  $0.5 \text{ s./step}$ . Experimental X-ray patterns were analyzed with the Powder Diffraction Files (PDF) from the database published by the International Centre for Diffraction Data (ICDD).

### 2.3. Determination of portlandite concentration with thermogravimetric analysis (TGA)

Thermogravimetric testing was carried out on powdered samples using an automated instrument (TGA-Q500, TA Instruments). Prior to

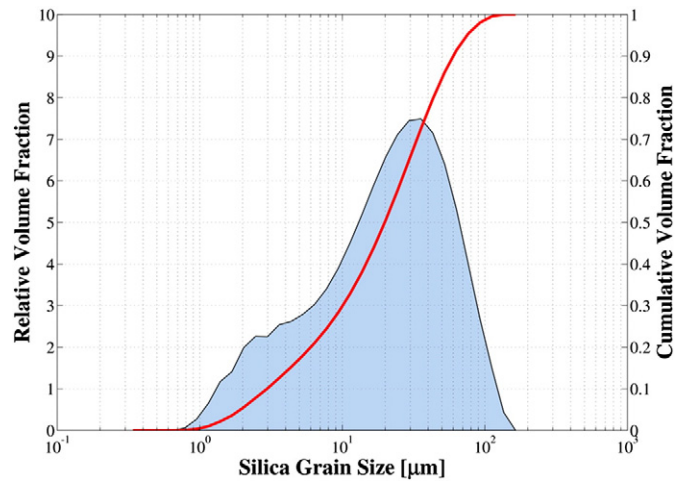


Fig. 1. Particle size distribution of the silica flour (ground quartz) incorporated into the A-series samples.

TGA analysis, samples were ground and dried at  $50^\circ\text{C}$  for 5 days in a vacuum oven. Approximately 16 mg of sample was heated at the rate of  $20^\circ\text{C/min}$ . The amount of free portlandite (CH) in each sample was determined according the following relationships [3]:

$$\text{Free Ca(OH)}_2 = 4.11C \quad (1)$$

$$\text{Total Ca(OH)}_2 = 4.11C + 1.68D \quad (2)$$

where C is the mass loss between  $440^\circ\text{C}$  and  $580^\circ\text{C}$ . The second reported value is the total amount of CH, which takes into account the eventual carbonation, Eq. (2), where D stands for the weight loss between  $580^\circ\text{C}$  and  $940^\circ\text{C}$  attributed to the decomposition of calcium carbonate (assumed to have formed from CH).

### 2.4. Nanoscale morphological analysis via transmission electron microscopy (TEM)

Imaging of fine, nanometer-scale microstructural features of selected samples was performed using a high-resolution transmission electron microscope (JEOL 2010, Tokyo, Japan). The cement samples were ground into a fine powder with a mortar and pestle, dried at  $60^\circ\text{C}$  for 6 h under vacuum, and then dispersed onto a standard TEM copper grid. Immediately after, the samples were examined under the electron probe.

The micrographs of characteristic lattice fringes were treated in the Scanning Probe Image Processor software, which includes image scaling and filtering with Fast Fourier Transform (FFT) [4]. The maximum FFT threshold was set to 50 while the minimum was kept at 0. Applying these threshold bounds considerably improved the signal-to-noise ratio of the image obtained from the inverse FFT transformation, and allowed for accurate measurements of the distance between the adjacent fringes of the crystal lattice. A minimum of 12 measurements were taken for quantitative analysis, each corresponding to the

Table 1  
Investigated cement systems: control neat system (J-series) and silica enriched system (A-series).

Label	J-30	J-85	J-130	A-30	A-60	A-85	A-110	A-130	A-175	A-200
w/c	0.45			0.45						
Silica (%)	–			35.0						
T ( $^\circ\text{C}$ )	30	85	130	30	60	85	110	130	175	200
P (MPa)	20.7			20.7						
t (h)	100	100	22/258/572	144	145	147	145	73/148	17/40/188	1 w/1 m/1 y

silica (%) – by weight of cement (bwoc), 1 w/1 m/1 y = week, month and year.

Download English Version:

<https://daneshyari.com/en/article/1456206>

Download Persian Version:

<https://daneshyari.com/article/1456206>

[Daneshyari.com](https://daneshyari.com)